Cancer Management and Research

Dovepress

open access to scientific and medical research

Open Access Full Text Article

ORIGINAL RESEARCH

RETRACTED ARTICLE: Long Noncoding RNA LINC01426 Sequesters microRNA-519d-5p to Promote Non-Small Cell Lung Cancer Progression by Increasing ETS1 Expression

This article was published in the following Dove Press journal:
Cancer Management and Research

Jixin Dai[1]
Bing Wang[2]
Yueming Zhao[1]
Xuerong Zuo[1]
Hongxia Cui[1]
Xi Chen[2]
Xianhong Liu[1]

[1]Department of Oncology, Jilin Cancer Hospital, Changchun, Jilin 130000, People's Republic of China; [2]Department of Radiotherapy, Jilin Cancer Hospital, Changchun, Jilin 130000, People's Republic of China

Purpose: Recent studies have identified important roles for *long intergenic non-protein coding RNA 1426* (*LINC01426*) in glioma and clear cell renal cell carcinoma. The present study evaluated the expression profile of *LINC01426* in non-small cell lung cancer (NSCLC) tissues and cell lines. Furthermore, the function of *LINC01426* in NSCLC and the molecular mechanisms involved were extensively studied.

Methods: The abundance of *LINC01426* in NSCLC tissues and cell lines was determined using quantitative reverse transcription–polymerase chain reaction. The cell counting kit-8 assay, flow cytometry, transwell experiments for migration and invasion, and xenograft tumor model were used to assess the function of *LINC01426* in NSCLC cells. Mechanistic studies were performed using dual-luciferase reporter assay and RNA immunoprecipitation.

Results: Significant *LINC01426* upregulation was observed in NSCLC tissues and cell lines. Silencing *LINC01426* inhibited proliferation, migration, and invasion of NSCLC cells and facilitated apoptosis in vitro. Furthermore, interference of *LINC01426* restricted tumor growth of NSCLC cells in vivo. In addition, *LINC01426* showed the ability to directly bind to microRNA-519d-5p (miR-519d-5p) and act as a molecular sponge for miR-519d-5p in NSCLC cells. Furthermore, the *ETS proto-oncogene 1* (*ETS1*) was identified as a direct target of miR-519d-5p and *LINC01426* could indirectly upregulate *ETS1* expression by sponging miR-519d-5p. Moreover, the cancer-inhibiting activities of *LINC01426* knockdown in NSCLC cells were partially offset by miR-519d-5p inhibition.

Conclusion: *LINC01426* increases *ETS1* expression by sequestering miR-519d-5p, thereby aggravating the malignant progression of NSCLC. The LINC01426/miR-519d-5p/ETS1 competing endogenous RNA pathway may provide a target for designing therapeutic agents for NSCLC treatment.

Keywords: long intergenic non-protein coding RNA 1426, NSCLC, ETS proto-oncogene 1, ceRNA

Introduction

Lung cancer is the most commonly diagnosed cancer and the leading cause of cancer-related mortality worldwide.[1] According to estimates, lung cancer will afflict 228,150 individuals and cause 147,510 deaths annually worldwide.[2] Non-small cell lung cancer (NSCLC), the most prominent type of lung cancer, accounts for approximately 80%–85% of all lung cancer diagnoses.[3] NSCLC comprises several pathological types, including squamous cell carcinoma, adenocarcinoma, and large cell carcinoma.[4] Over

Correspondence: Xianhong Liu
Department of Oncology, Jilin Cancer Hospital, 1018 Huguang Road, Changchun, Jilin 130000, People's Republic of China
Email liuxianhong_onc@163.com

submit your manuscript | www.dovepress.com
DovePress
http://doi.org/10.2147/CMAR.S277113

the past few decades, with progress in diagnostic techniques and therapeutic regimens, the clinical outcome for NSCLC has substantially improved.[5] However, the prognosis for NSCLC remains dismal as the 5-year survival rate is only 19.7%.[6] Recurrence, metastasis, and drug resistance lead to poor clinical outcomes for NSCLC.[7] NSCLC exhibits complicated biological characteristics, involving multiple pathophysiological changes, and gene and molecular pathway dysregulation.[8] Consequently, the underlying mechanisms remain elusive and require further exploration. Therefore, elucidating the molecular events responsible for NSCLC pathogenesis will be useful for improving diagnosis and treatment.

Long noncoding RNAs (lncRNAs) are transcripts consisting of >200 nucleotides.[9] They lack protein coding capacity and have attracted increased attention over the past decade.[10] Furthermore, lncRNAs are implicated in the control of several physiological processes, such as genomic imprinting, chromatin organization, immunoregulation, cell cycle, and differentiation.[11,12] Compelling studies have revealed that numerous lncRNAs are aberrantly expressed in various human malignancies and affect cell biological processes associated with cancer.[13–15] In NSCLC, lncRNAs have emerged as novel regulators of oncogenesis and cancer progression and they contribute to the malignant phenotype.[16–18]

MicroRNAs (miRNAs) are a cluster of highly conserved, single-stranded, short noncoding RNA transcripts composed of 17–25 nucleotides.[19] These molecules are capable of negatively regulating gene expression via base pairing with the 3′-untranslated regions (3′-UTRs) of target mRNAs. This triggers mRNA degradation and translation repression.[20] The differentially expressed miRNAs can regulate the oncogenicity of NSCLC by executing tumor-promoting or tumor-inhibiting roles.[21,22] In recent years, the competing endogenous RNA (ceRNA) theory has been proposed and gradually be adopted.[23] This theory asserts that lncRNAs function as ceRNAs by decoying specific miRNAs, thereby abolishing the miRNA-mediated target mRNA degradation.[24] Therefore, elucidating the detailed functions of cancer-associated lncRNAs in NSCLC will contribute to cancer intervention and therapy.

Recent studies have identified the important roles for *LINC01426* in glioma,[25,26] clear cell renal cell carcinoma,[27] and lung adenocarcinoma.[28] However, studies on the expression profile and functions of *LINC01426* in NSCLC are limited. Therefore, the main aim of our study was to detect the expression profile for *LINC01426* in NSCLC tissues and cell lines. Furthermore, the function of *LINC01426* in NSCLC and the related molecular mechanisms involved were investigated.

Materials and Methods

Tissue Sample Collection

A total of 58 pairs of NSCLC tissues and corresponding adjacent normal tissues were obtained from patients at the Jilin Cancer Hospital. None of the patients had previously received preoperative radiotherapy, chemotherapy, or other anticancer treatments, and none experienced any other acute or chronic diseases or cancers. Tissues were stored in liquid nitrogen until further use. The Ethics Committee of Jilin Cancer Hospital (2017-0216) reviewed and approved this study. The study was conducted in accordance with the Declaration of Helsinki and all tissue samples were obtained with written informed consent.

Cell Culture

The human non-tumorigenic bronchial epithelial cell line, BEAS-2B, was obtained from the American Type Culture Collection (ATCC; Manassas, VA, USA) and cultured in Bronchial Epithelial Cell Growth Medium (Lonza/Clonetics Corporation, Walkersville, MD, USA). Two NSCLC cell lines, H522 and H460, were also obtained from the ATCC and maintained in RPMI 1640 medium (Gibco; Thermo Fisher Scientific, Inc., Waltham, MA, USA) supplemented with 10% fetal bovine serum (FBS; Gibco; Thermo Fisher Scientific, Inc.) and 1% penicillin/streptomycin (Gibco; Thermo Fisher Scientific, Inc.). The other two NSCLC cell lines, SK-MES-1 and A549, were purchased from the Cell Bank of the Chinese Academy of Sciences (Shanghai, China). A549 cells were cultured in F-12K medium (Gibco; Thermo Fisher Scientific, Inc.) containing 10% FBS, 1% Glutamax, and 1% penicillin/streptomycin. Minimum essential medium (Gibco; Thermo Fisher Scientific, Inc.) containing 10% FBS, 1% Glutamax, 1% Non-essential Amino Acids (Gibco; Thermo Fisher Scientific, Inc.), 1% sodium pyruvate solution (100 mM,Gibco; Thermo Fisher Scientific, Inc.), and 1% penicillin/streptomycin was added to the SK-MES-1 cell culture. All aforementioned cells were grown in a sterilized incubator at 37°C supplemented with 5% CO_2.

Oligonucleotides, Plasmids, and Cell Transfection

The miR-519d-5p mimic, negative control (NC) miRNA mimic (miR-NC), miR-519d-5p inhibitor (anti-miR-519d-5p), and NC inhibitor (anti-NC) were produced by RiboBio

Co., Ltd (Guangzhou, China). The small interfering RNAs (siRNAs) that target *LINC01426* expression (si-LINC01426) and NC expression (si-NC) were designed and synthesized by Genepharma Co., Ltd (Shanghai, China). The *ETS1* overexpressing plasmid, pcDNA3.1-ETS1, was constructed by the Shanghai Sangon Company (Shanghai, China). NSCLC cells were seeded into 6-well plates and grown to 70%–80% confluence before being transiently transfected with oligonucleotides or plasmids using Lipofectamine 2000 (Invitrogen; Thermo Fisher Scientific, Inc.).

RNA Preparation and Quantitative Reverse Transcription–Polymerase Chain Reaction (qRT-PCR)

Total RNA extraction was performed using TRIzol reagent (KeyGEN BioTECH; Nanjing, China). A NanoDrop 2000c spectrophotometer (Invitrogen; Thermo Fisher Scientific, Inc.) was used for determining the quality and quantity of total RNA. Total RNA was reverse transcribed into complementary DNA (cDNA) using a Mir-X miRNA First-Strand Synthesis Kit (Takara, Dalian, China). Quantitative PCR was then performed to detect miR-519d-5p expression using a Mir-X miRNA qRT-PCR TB Green® Kit (Takara). To quantitate *LINC01426* and *ETS1* expression, a QuantiTect Reverse Transcription Kit (Qiagen GmbH, Hilden, Germany) was employed for cDNA synthesis. Thereafter, a QuantiTect SYBR Green PCR Kit (Qiagen GmbH) was used for quantitative PCR. *GAPDH* acted as an endogenous control for *LINC01426* and *ETS1*, whereas miR-519d-5p expression was normalized to that of *U6* small nuclear RNA. All gene expression measurements were calculated using the $2^{-\Delta\Delta Cq}$ method. Each sample was measured in triplicate, and the same experiment was repeated three times.

Cell Counting Kit-8 (CCK-8) Assay

Transfected cells were detached with 0.25% trypsin at 24 h post-transfection, centrifuged, and resuspended in complete culture medium at a density of 2×10^4 cells/mL. Each well of the 96-well plates was administered 100 µL cell suspension, and 5 replicate wells were established for each group. After cultivating for 0, 24, 48, and 72 h, 10 µL CCK-8 solution (Dojindo Laboratories, Kumamoto, Japan) was added, and the plates were incubated at 37°C with 5% CO_2 for 2 h. The absorbance at 450 nm was measured using a microplate reader (Tecan Group, Ltd., Mannedorf, Switzerland).

Flow Cytometry

An Annexin V-FITC Apoptosis Detection Kit (Beyotime; Shanghai, China) was used in the assessment of cell apoptosis. Briefly, transfected cells were cultured for 48 h, detached using EDTA-free trypsin, and centrifugated at 1000 ×g for 5 min at 4°C, followed by resuspending in 195 µL binding buffer. Thereafter, 5 µL Annexin-V-FITC and 10 µL PI were added to the cell suspension. After 20-min incubation at 25°C in the dark, cell apoptosis was detected using a flow cytometer (BD Biosciences, Franklin Lakes, NJ, USA). All data were analyzed using a BD FACSCanto™ system software v2.4 (BD Biosciences).

Transwell Experiments for Migration and Invasion

Cell migration and invasion were evaluated in transwell experiments. For the migration assay, 1×10^5 cells were resuspended in serum-free culture medium and plated into the upper compartment of the transwell chambers (BD Biosciences). The lower chambers were loaded with 600 µL culture medium supplemented with 20% FBS. After 24 h, the cells remaining on the upper surface of the membranes were removed using a cotton swab. The migrated cells were fixed with 4% paraformaldehyde and then stained with 0.1% crystal violet. These cells were visualized using an inverted light microscope (Olympus Corporation, Tokyo, Japan). A total of six fields of view were arbitrarily selected and the cell numbers were counted. The experimental procedure for the invasion assay were the same as the migration assay, except that the transwell chambers were precoated with Matrigel (BD Biosciences).

Tumor Xenografts

All animal experiments were conducted following the NIH guidelines for the care and use of laboratory animals and approved by the Animal Experimental Ethics Committee of Jilin Cancer Hospital (2018–1102). Male BALB/c nude mice (4–6 weeks old) were obtained from the Beijing Vital River Laboratory Animal Technology Co., Ltd. (Beijing, China) and housed under specific pathogen-free conditions. The lentivirus stably expressing short hairpin RNA (shRNA) against *LINC01426* (sh-LINC01426) and NC (sh-NC) were designed and prepared by Genepharma Co., Ltd.

H460 cells were transduced with lentivirus and treated with puromycin to obtain a stable cell line. A total of 6

mice were used in animal experiments, and were randomly divided into groups sh-LINC01426 and sh-NC. H460 cells stably overexpressing sh-LINC01426 were subcutaneously injected into the flanks of nude mice in sh-LINC01426 group, whereas the sh-NC group was subcutaneously injected with H460 cells stably overexpressing sh-NC. Tumor width and length were weekly monitored using a Vernier caliper, and the tumor volume was calculated as follows: tumor volume = 0.5 × (length × width^2). After 4 weeks, the nude mice were euthanized by cervical dislocation, the tumor xenografts were removed, weighed, and used for subsequent assays.

Bioinformatics Analysis

The miRDB database (http://mirdb.org/) was used to identify miRNAs that may interact with *LINC01426*. The putative targets of miR-519d-5p were predicted using the miRDB (http://mirdb.org/) and TargetScan (http://www.targetscan.org/) programs.

RNA Immunoprecipitation (RIP) Assay

RIP assay was performed to detect the binding between *LINC01426* and miR-519d-5p using a Magna RIP RNA-Binding Protein Immunoprecipitation kit (EMD Millipore). NSCLC cells were lysed in RIP buffer, and the cell extracts were incubated with magnetic beads conjugated with anti-Ago2 antibody (Millipore) or normal *IgG* (Millipore). Prior to immunoprecipitated RNA extraction, the magnetic beads were harvested and overnight incubation at 4°C, rinsed with RIP wash buffer, and treated with proteinase K to remove protein. The immunoprecipitated RNA was measured using qRT-PCR.

Nuclear–Cytoplasmic Fractionation Assay

Nuclear and cytoplasmic fractions were separated using the Cytoplasmic and Nuclear RNA Purification Kit (Norgen, Belmont, CA, USA). The RNA in both fractions was extracted and subjected to qRT-PCR analysis for determining the distribution of *LINC01426*.

Luciferase Reporter Assay

The *LINC01426* and *ETS1* 3′-UTR fragments containing the miR-519d-5p binding site were amplified and cloned into the pmirGLO luciferase vector (Promega Corporation, Madison, WI, USA). The produced luciferase reporter vectors were termed as LINC01426-wild-type (LINC01426-wt) and ETS1-wt. Mutated *LINC01426* and *ETS1* 3′-UTR fragments with disruption in the putative miR-519d-5p binding sequences were generated using a QuikChange Site-Directed Mutagenesis Kit (Stratagene, La Jolla, CA, USA). Further, the mutated fragments were inserted into the pmirGLO luciferase vector to obtain the LINC01426-mutant (LINC01426-mut) and ETS1-mut reporter vectors. NSCLC cells were seeded into 6-well plates and cotransfected with miR-519d-5p mimic or miR-NC and wt or mut reporter vectors using Lipofectamine 2000. At 48 h after transfection, the Dual Luciferase Reporter Assay System (Promega Corporation) was used to detect the activity of firefly luciferase, which was normalized to that of Renilla luciferase.

Western Blot Analysis

Cultured cells were rinsed with phosphate buffer solution, and total protein was isolated using RIPA buffer (KeyGEN BioTECH). Following quantification using a BCA protein assay kit (KeyGEN BioTECH), equal amounts of protein were separated on 10% sodium dodecyl sulfate polyacrylamide gels. The separated proteins were then transferred to polyvinylidene fluoride membranes (Millipore), blocked with 5% non-fat milk at room temperature for 2 h and incubated overnight with primary antibodies against *ETS1* (ab220361; Abcam, Cambridge, UK) or *GAPDH* (ab181602; Abcam). Goat anti-rabbit IgG-HRP secondary antibody (ab205718; Abcam) was incubated with the membranes. Thereafter, an ECL detection kit (KeyGEN BioTECH) was used for the development of protein signals.

Statistical Analysis

All experiments were repeated thrice, and the data were presented as the means ± standard deviations. The differences between two groups were determined by a Student's *t*-test. One-way ANOVA, followed by Tukey's post-hoc test, was used to determine the differences among multiple groups. The correlations among *LINC01426*, miR-519d-5p, and *ETS1* expression in the NSCLC tissues were evaluated using Pearson's correlation analysis. All statistical analyses were performed using SPSS19.0 software (SPSS Inc., USA). A P value of <0.05 was considered statistically significant.

Results

LINC01426 is Highly Expressed in NSCLC Tissues and Cell Lines

LINC01426 expression in lung adenocarcinoma (LUAD) and lung squamous cell carcinoma (LUSC) was analyzed using TCGA dataset. The results indicated that *LINC01426* was clearly elevated in LUAD and LUSC (Figure 1A). Further,

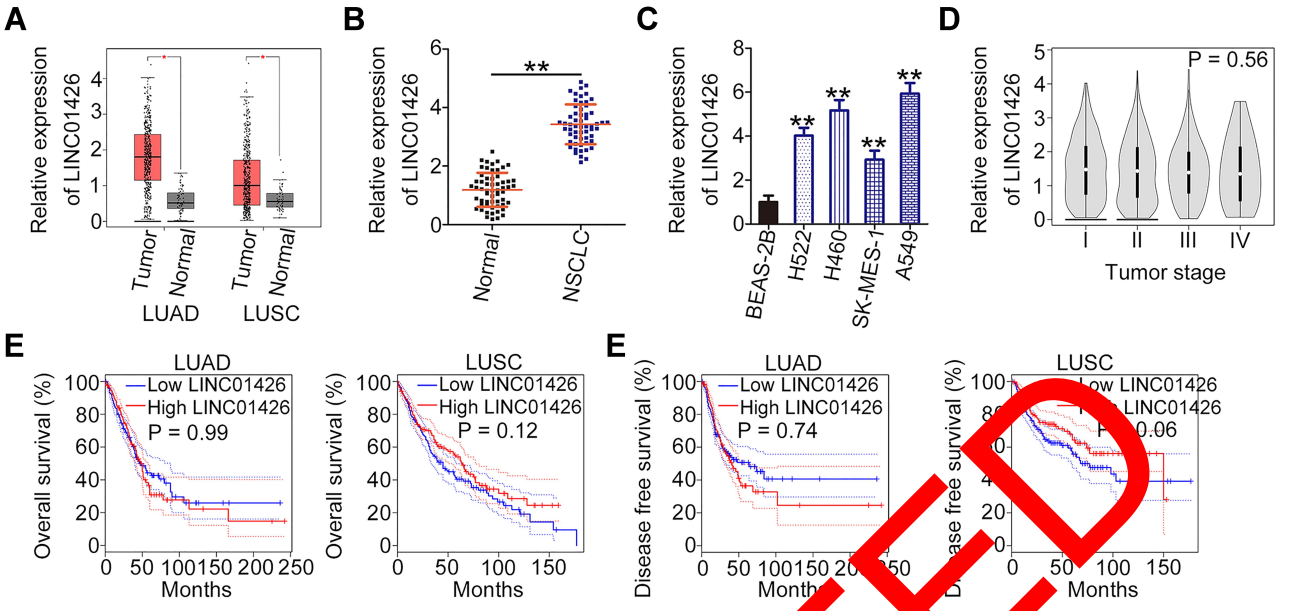

Figure 1 *LINC01426*is highly expressed in NSCLC tissues and cell lines. (**A**) The TCGA dataset was used to analyze *LINC01426* expression in LUAD and LUSC. (**B**) *LINC01426* expression in 58 pairs of NSCLC tissues and corresponding adjacent normal tissues was measured using qRT-PCR. (**C**) *LINC01426* expression in NSCLC cell lines (H522, H460, SK-MES-1 and A549) was measured using qRT-PCR. A human non-tumorigenic bronchial epithelial cell line BEAS-2B was used as control. (**D**) The correlation between *LINC01426* expression and tumor stage in LUAD and LUSC was analyzed using the TCGA dataset. (**E, F**) The correlation between *LINC01426* expression and overall survival or disease-free survival in LUAD and LUSC was determined using the TCGA dataset. $^{**}P < 0.01$.

a total of 58 pairs of NSCLC tissues and corresponding adjacent normal tissues were collected and analyzed using qRT-PCR to determine *LINC01426* expression. *LINC01426* expression was higher in NSCLC tissues compared with that in the adjacent normal tissues (Figure 1B). Similarly, *LINC01426* expression in NSCLC cell lines (H522, H460, SK-MES-1 and A549) was significantly upregulated compared with that in the human non-tumorigenic bronchial epithelial cell line BEAS-2B (Figure 1C). Re-analyzing the TCGA dataset along with available survival data revealed no correlation between *LINC01426* expression and tumor stage in either LUAD or LUSC (Figure 1D). Furthermore, a high *LINC01426* expression was not associated with either overall survival (Figure 1E) or disease-free survival (Figure 1F) in patients with LUAD and LUSC. These results indicate that *LINC01426* is upregulated in NSCLC.

LINC01426 Depletion Inhibits NSCLC Cell Proliferation, Migration, and Invasion and Promotes Cell Apoptosis in vitro

LINC01426 expression was most abundant in the cell lines H460 and A549; therefore, they were selected for experimental use. To further elucidate the role of *LINC01426* in NSCLC, si-LINC01426 was transfected into H460 and A549 cells. *LINC01426* expression was decreased in H460 and A549 cells after si-LINC01426 transfection. Of the constructs, si-LINC01426#1 was the most effective and thus selected for functional experiments (Figure 2A). Using CCK-8 assay, our results revealed that *LINC01426* depletion inhibited the proliferation of H460 and A549 cells (Figure 2B). Additionally, *LINC01426* silencing increased apoptosis in H460 and A549 cells (Figure 2C). Furthermore, si-LINC01426 transfection resulted in reduced migration (Figure 2D) and invasion (Figure 2E) of H460 and A549 cells. Overall, *LINC01426* exerts oncogenic activity in NSCLC cells.

LINC01426 Acts as a ceRNA in NSCLC Cells by Sponging miR-519d-5p

To determine the manner in which *LINC01426* affects the oncogenicity of NSCLC cells, lncATLAS (http://lncatlas.crg.eu/) was used to predict the subcellular localization of *LINC01426*. The results indicated that *LINC01426* was primarily enriched in the cytoplasm (Figure 3A). A nuclear–cytoplasmic fractionation assay coupled with qRT-PCR analysis further confirmed this observation (Figure 3B), suggesting that *LINC01426* is implicated in NSCLC progression via a ceRNA mechanism. A bioinformatics analysis revealed a total of 22 miRNAs that were capable of complementary base pairing with *LINC01426* (Figure 3C). Among these candidates, miR-519d-5p,[29] miR-873-3p,[30,31] miR-377-5p,[32,33] and miR-548c-3p[34,35] were selected for experimental

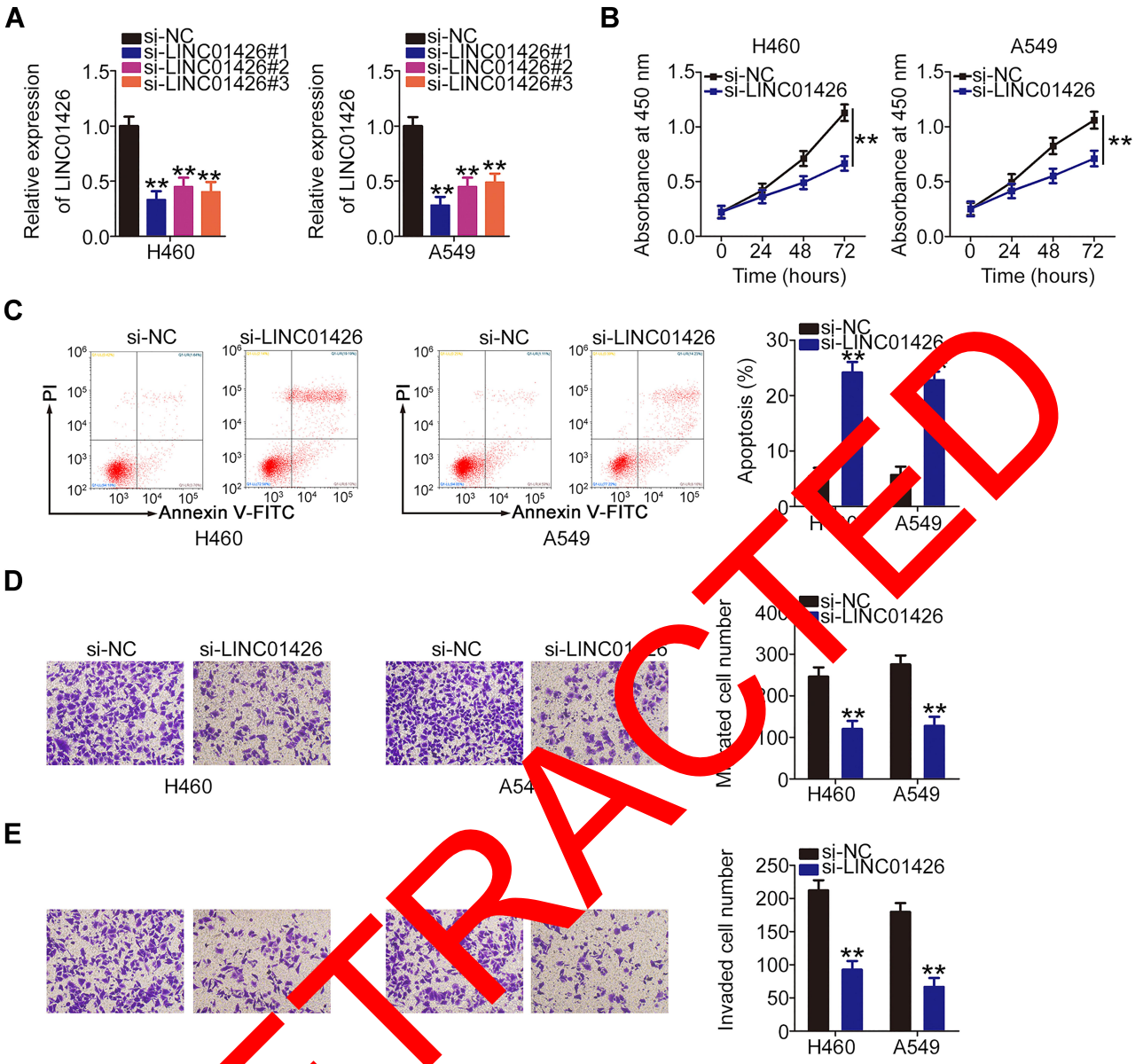

Figure 2 *LINC01426* knockdown inhibits NSCLC cell proliferation, migration, and invasion and promotes cell apoptosis in vitro. (**A**) *LINC01426* expression was measured in H460 and A549 cells using qRT-PCR after si-LINC01426 or si-NC transfection. (**B**) CCK-8 assay was performed to assess the proliferation of LINC01426-deficient H460 and A549 cells. (**C**) Flow cytometry was performed to evaluate the effect of *LINC01426* depletion on apoptosis in H460 and A549 cells. (**D, E**) The migratory and invasive capacities of H460 and A549 cells following *LINC01426* silencing were determined by transwell experiments. **P < 0.01.

verification before they played critical functions in various human cancers.

Following *LINC01426* interference, qRT-PCR analysis was performed to detect the expression of the four miRNAs in H460 and A549 cells. It was found that miR-519d-5p expression was significantly increased in *LINC01426* deficient-H460 and -A549 cells (Figure 3D). By contrast, the expression of other three miRNAs remained unchanged following si-LINC01426 transfection. In addition, miR-519d-5p expression was reduced in NSCLC tissues compared with that in the adjacent normal tissues (Figure 3E). Data from Pearson's correlation analysis revealed an inverse correlation between *LINC01426* and miR-519d-5p levels in the 58 NSCLC tissues (Figure 3F; $r = -0.7313$, $P < 0.0001$).

Figure 3G depicts the binding sequence of miR-519d-5p within the sequence of *LINC01426*. To further validate this prediction, the luciferase reporter assay was conducted to address the binding interaction between *LINC01426* and miR-519d-5p in NSCLC cells. The miR-519d-5p mimic transfection was detected using qRT-PCR. In miR-519d-5p mimic-transfected H460 and A549 cells, miR-519d-5p showed marked overexpression (Figure 3H). The luciferase

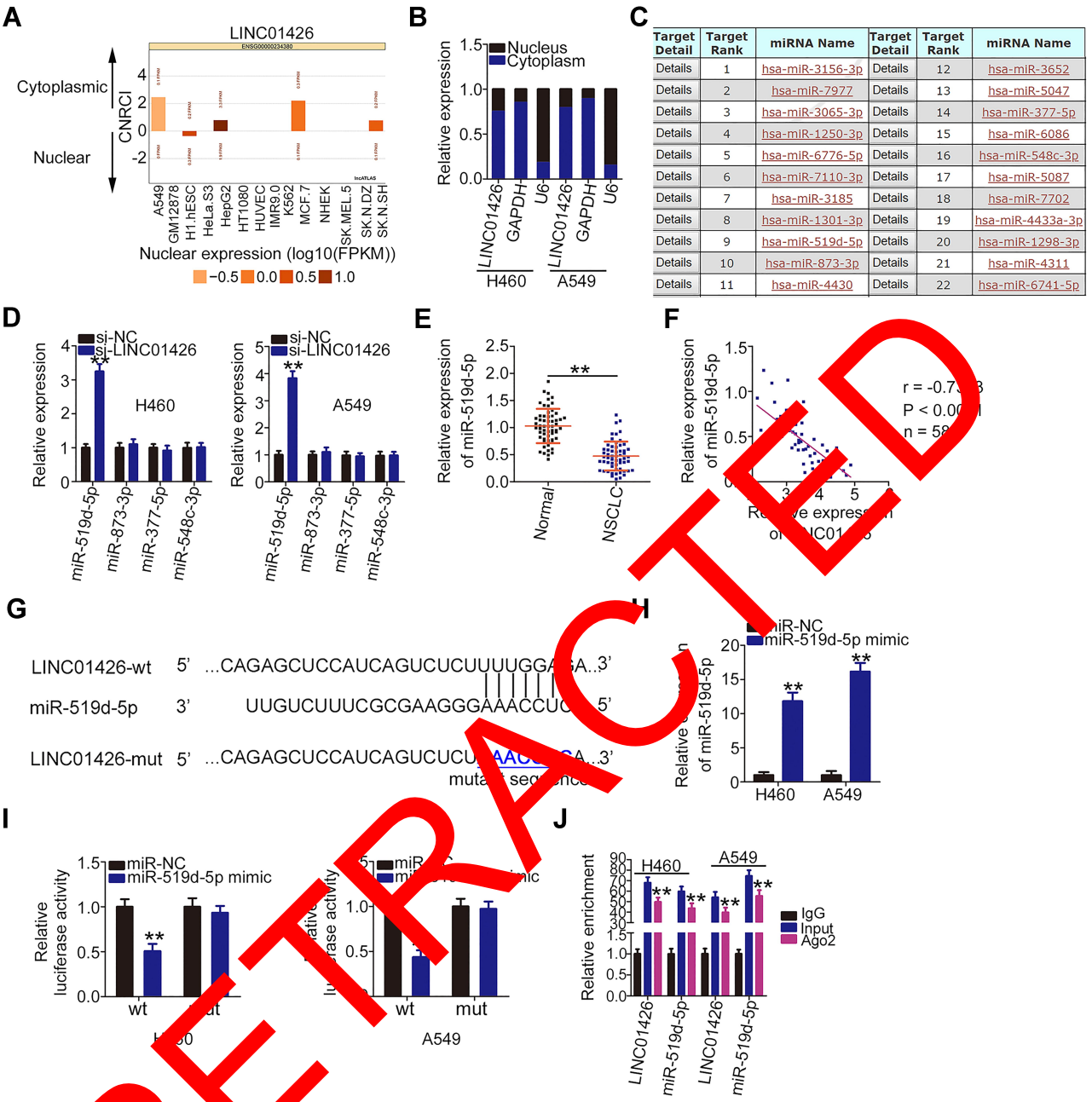

Target Detail	Target Rank	miRNA Name	Target Detail	Target Rank	miRNA Name
Details	1	hsa-miR-3156-3p	Details	12	hsa-miR-3652
Details	2	hsa-miR-7977	Details	13	hsa-miR-5047
Details	3	hsa-miR-3065-3p	Details	14	hsa-miR-377-5p
Details	4	hsa-miR-1250-3p	Details	15	hsa-miR-6086
Details	5	hsa-miR-6776-5p	Details	16	hsa-miR-548c-3p
Details	6	hsa-miR-7110-3p	Details	17	hsa-miR-5087
Details	7	hsa-miR-3185	Details	18	hsa-miR-7702
Details	8	hsa-miR-1301-3p	Details	19	hsa-miR-4433a-3p
Details	9	hsa-miR-519d-5p	Details	20	hsa-miR-1298-3p
Details	10	hsa-miR-873-3p	Details	21	hsa-miR-4311
Details	11	hsa-miR-4430	Details	22	hsa-miR-6741-5p

Figure 3 *LINC01426* is a molecular sponge for miR-519d-5p in NSCLC cells. (**A**) The subcellular localization of *LINC01426* was predicted by lncATLAS. (**B**) Nuclear–cytoplasm fractionation was conducted to evaluate the distribution of *LINC01426* in H460 and A549 cells. (**C**) The putative miRNAs that interact with *LINC01426* were predicted by miRDB. (**D**) miR-519d-5p, miR-873-3p, miR-377-5p, and miR-548c-3p expression levels in H460 and A549 cells after *LINC01426* knockdown was determined using qRT-PCR. (**E**) qRT-PCR was performed to detect miR-519d-5p expression in 58 pairs of NSCLC tissues and corresponding adjacent normal tissues. (**F**) Pearson's correlation analysis was conducted to address the correlation between *LINC01426* and miR-519d-5p expression in the 58 NSCLC tissues. (**G**) The putative binding sequence of miR-519d-5p within the sequence of *LINC01426* was determined via a bioinformatics analysis, and the mutant binding sequences are shown. (**H**) The transfection efficiency of the miR-519d-5p mimic in increasing endogenous miR-519d-5p expression in H460 and A549 cells was measured using qRT-PCR. (**I**) Luciferase activity was measured in H460 and A549 cells following miR-519d-5p mimic or miR-NC transfection and LINC01426-wt or LINC01426-mut transfection. (**J**) RIP assay was employed to assess the enrichment of miR-519d-5p and *LINC01426* in the anti-Ago2 or anti-IgG precipitates. **P < 0.01.

activity of LINC01426-wt was lower in response to miR-519d-5p upregulation, whereas the activity of LINC01426-mut showed no significant change following miR-519d-5p mimic cotransfection (Figure 3I). RIP assay further confirmed this result considering that *LINC01426* and miR-519d-5p were immunoprecipitated by anti-Ago2 antibody (Figure 3J), indicating the coexistence of *LINC01426* and miR-519d-5p in the same RNA-induced silencing complex. Collectively, these findings suggest that *LINC01426* functions as a ceRNA in NSCLC cells by sponging miR-519d-5p.

miR-519d-5p is an Anti-Oncogenic miRNA That Directly Targets ETS1 in NSCLC Cells

Using bioinformatics tools, *ETS1* (Figure 4A) was identified and selected for further confirmation because of its oncogenic effects in the malignant properties of NSCLC cells.[36–38] Results of the luciferase reporter assay revealed that miR-519d-5p overexpression significantly inhibited the luciferase activity of ETS1-wt in H460 and A549 cells, whereas the inhibitory effect was abrogated when the binding sequences were mutated (Figure 4B). Moreover, miR-519d-5p upregulation negatively affected *ETS1* mRNA (Figure 4C) and protein (Figure 4D) expression in H460 and A549 cells. Furthermore, *ETS1* was significantly overexpressed in NSCLC tissues compared with that in the adjacent normal tissues (Figure 4E). Importantly, an inverse correlation was observed between the levels of miR-519d-5p and *ETS1* in the 58 NSCLC tissues (Figure 4F; r = −0.6239, P < 0.0001). In summary, miR-519d-5p directly targets *ETS1* and inhibits NSCLC progression.

LINC01426 Exerts Oncogenic Activity in NSCLC by Regulating the miR-519d-5p/ETS1 Axis

LINC01426 was verified as an miR-519d-5p sponge, and miR-519d-5p directly targeted *ETS1* in NSCLC cells. The above experimental results further suggest that *LINC01426* can regulate *ETS1* expression in NSCLC cells by competitively binding to miR-519d-5p. Accordingly, *ETS1* mRNA and protein levels in LNC01426-depleted H460 and A549 cells were measured using qRT-PCR and Western blot assays. The results revealed that *ETS1* expression was significantly inhibited in H460 and A549 cells when *LINC01426* was silenced (Figure 5A and B). However, anti-miR-519d-5p (Figure 5C) cotransfection reversed these regulatory effects (Figure 5D and E). The Pearson's correlation analysis revealed a positive correlation between *LINC01426* and *ETS1* mRNA levels in NSCLC tissues (Figure 5F; r = 0.6636, P < 0.0001). Subsequently, rescue experiments were performed by knocking down miR-519d-5p expression in LNC01426-depleted H460 and A549 cells. Functional experiments demonstrated that miR-519d-5p inhibition abolished the si-LINC01426-mediated effects on cell proliferation (Figure 5G) and apoptosis (Figure 5H) of H460 and A549 cells. Furthermore, although the migratory (Figure 5I) and invasive (Figure 5J) capacities of H460 and A549 cells were decreased by *LINC01426* downregulation, they were restored following miR-519d-5p inhibition. Cumulatively, the miR-519d-5p/ETS1 axis functions as a downstream effector of *LINC01426* in promoting oncogenesis in NSCLC.

LINC01426 Silencing Inhibits NSCLC Cell Growth in vivo

To determine the effect of *LINC01426* on NSCLC cell growth in vivo, a xenograft model was established by injecting H460 cells stably overexpressing sh-LINC01426 or sh-NC into nude mice. The mice in the sh-

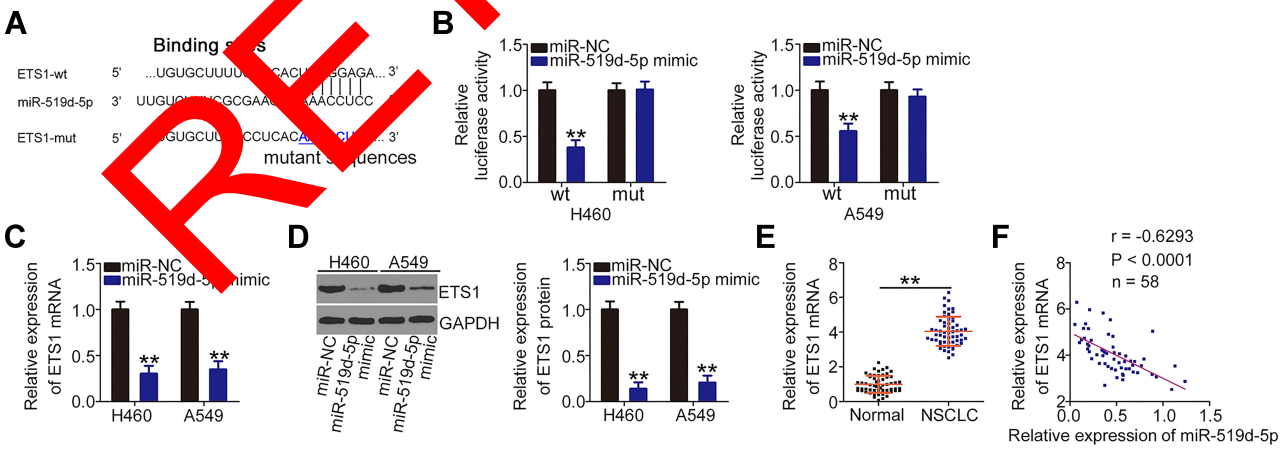

Figure 4 MiR-519d-5p directly targets *ETS1* in NSCLC cells. (**A**) The predicted miR-519d-5p binding site within the *ETS1* 3′-UTR and corresponding mutated site. (**B**) ETS1-wt or ETS1-mut and miR-519d-5p mimic or miR-NC were transfected into H460 and A549 cells. Luciferase activity was analyzed after 48-h incubation. (**C, D**) qRT-PCR and Western blot analysis were performed to measure the *ETS1* mRNA and protein levels, respectively, in miR-519d-5p mimic-transfected or miR-NC-transfected H460 and A549 cells. (**E**) *ETS1* mRNA expression in 58 pairs of NSCLC tissues and corresponding adjacent normal tissues was measured using qRT-PCR. (**F**) The correlation between miR-519d-5p and *ETS1* mRNA in 58 NSCLC tissues was analyzed by Pearson's correlation analysis. **P < 0.01.

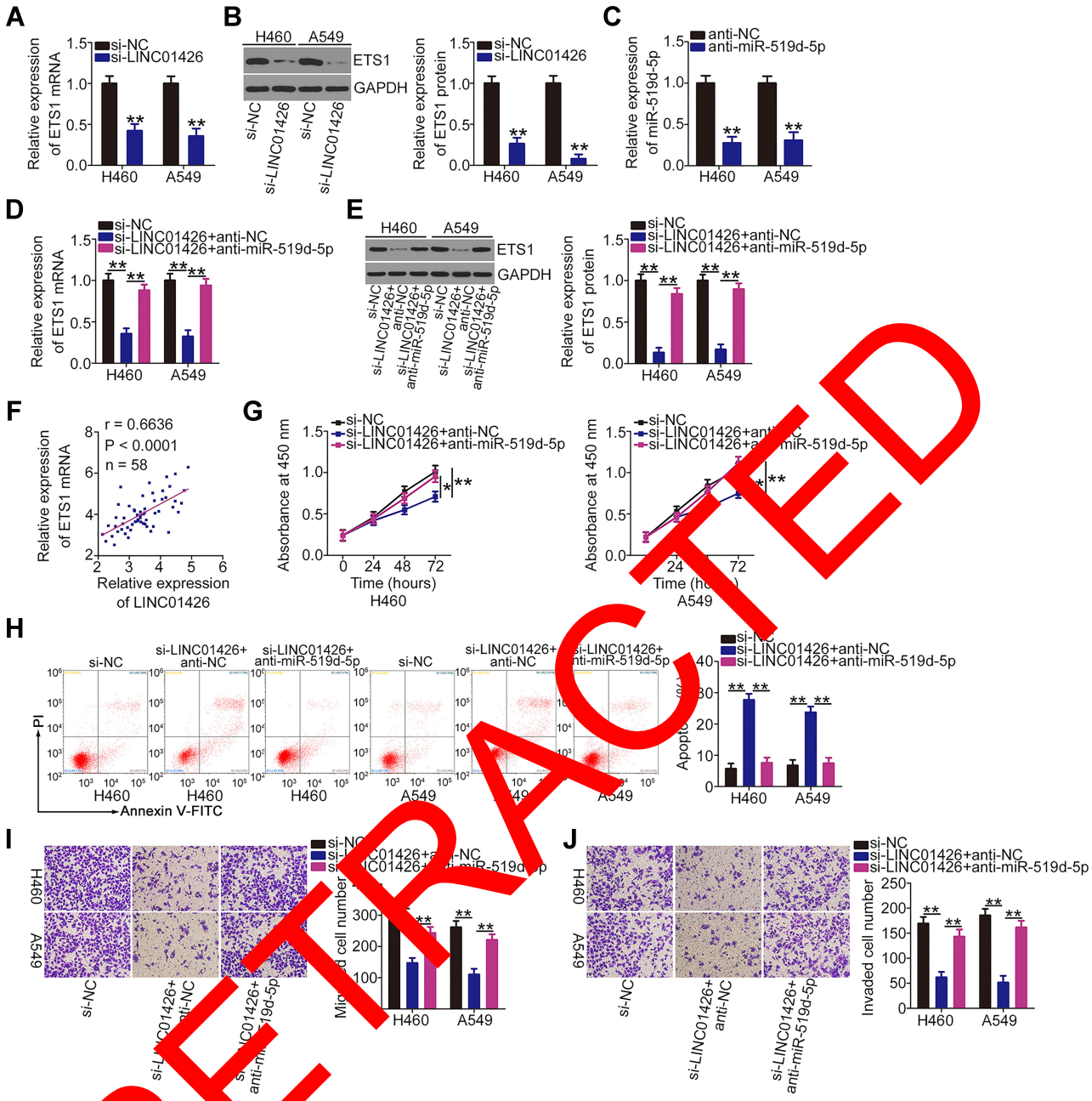

Figure 5 *LINC01426* exerts oncogenic activity in NSCLC cells by regulating the miR-519d-5p/ETS1 axis. (**A, B**) *ETS1* mRNA and protein levels in LINC01426-depleted H460 and A549 cells were examined using qRT-PCR and Western blot analysis, respectively. (**C**) qRT-PCR was used to assess the transfection efficiency of anti-miR-519d-5p in H460 and A549 cells. (**D, E**) H460 and A549 cells were transfected with anti-miR-519d-5p or anti-NC in the presence of si-LINC01426. qRT-PCR and Western blot analysis were performed to measure *ETS1* mRNA and protein expression levels, respectively. (**F**) Pearson's correlation analysis was conducted to assess the relationship between *LINC01426* and *ETS1* expression in 58 NSCLC tissues. (**G-J**) Anti-miR-519d-5p or anti-NC along with si-LINC01426 was introduced into H460 and A549 cells. The CCK-8 assay, flow cytometry, and transwell experiments for migration and invasion were conducted to determine cell proliferation, apoptosis, and migration and invasion, respectively. *P < 0.05 and **P < 0.01.

LINC01426 group exhibited decreased tumor volume (Figure 6A and B) and weight (Figure 6C) compared with the sh-NC group. *LINC01426* and miR-519d-5p expression levels in the tumor xenografts were measured using qRT-PCR. *LINC01426* was downregulated (Figure 6D) and miR-519d-5p was upregulated (Figure 6E) in the H460 tumor xenografts derived from *LINC01426* knockdown. Furthermore, the *ETS1* mRNA (Figure 6F) and protein (Figure 6G) expression levels were decreased in the LINC01426-depleted tumor xenografts. Collectively, these data indicate that *LINC01426* downregulation suppresses the growth of NSCLC tumors in vivo.

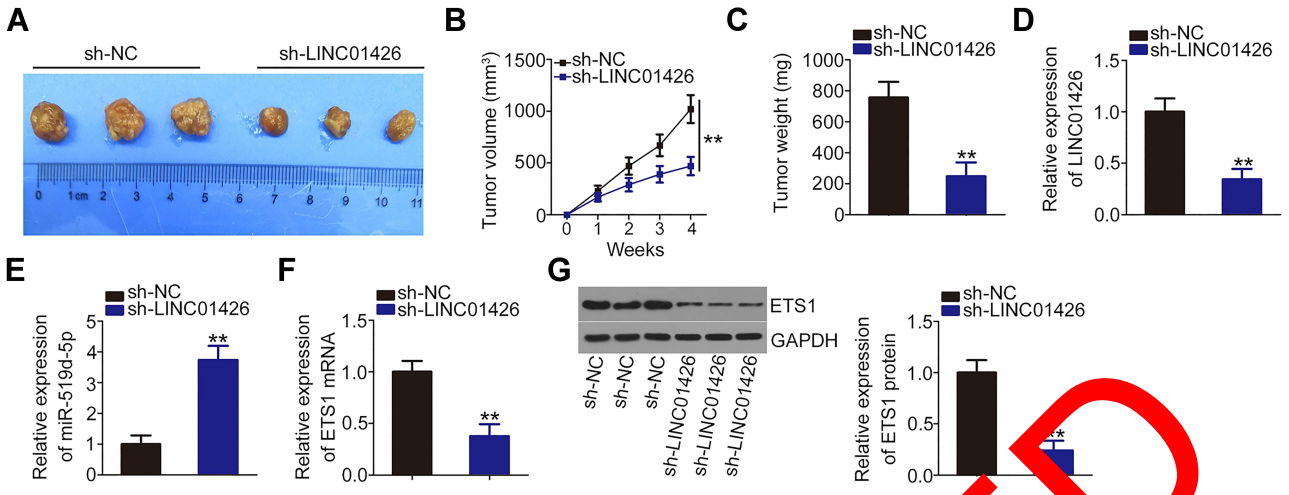

Figure 6 *LINC01426* knockdown inhibits the growth of NSCLC tumors in vivo. (**A**) After 28 days post-inoculation, mi[illegible] were euthanized a[illegible] xenografts were dissected and photographed. (**B**) Tumor volume was weekly recorded and growth curves were plotted. (**C**) Tumor xe[illegible]afts from [illegible] sh-LINC01[illegible]6 and sh-NC groups were weighed after removal. (**D**) *LINC01426* expression in the tumor xenografts was measured using qRT-PCR. (**E, F**) miR[illegible]9d-5[illegible]d *ETS1* mRNA expression levels were measured using qRT-PCR. (**G**) Western blot analysis of *ETS1* protein expression in tumor xenografts obtained fr[illegible] the sh-L[illegible]01426 and [illegible]NC groups. **P < 0.01.

Discussion

A significant body of evidence has indicated that lncRNAs are aberrantly expressed in NSCLC, which results in cancer progression, unlimited growth, and metastasis.[39–41] Moreover, lncRNAs have been identified as contributors to NSCLC etiology and development.[42,43] Therefore, investigating the regulatory activities of lncRNAs in NSCLC may lead to the identification of diagnostic markers and therapeutic targets for this fatal disease. However, the expression profile, detailed function, and regulatory mechanisms of most lncRNAs in NSCLC have not been elucidated. In the present study, we determined whether *LINC01426* is dysregulated in NSCLC and whether it could regulate NSCLC progression.

The expression and function of *LINC01426* in human cancers have recently attracted considerable interest. *LINC01426* is upregulated in glioma,[25] clear cell renal cell carcinoma,[27] and lung adenocarcinoma,[28] and elevated *LINC01426* expression is associated with adverse clinicopathological characteristics.[27,28] In addition, *LINC01426* is reportedly an independent predictor of prognosis in glioma.[25] Functionally, *LINC01426* exerts pro-oncogenic activities in glioma,[25,26] clear cell renal cell carcinoma,[27] and lung adenocarcinoma,[28] and it is implicated in the regulation of multiple tumor biological phenotypes. Therefore, the effect of *LINC01426* on the malignant phenotype of NSCLC warranted investigation. In the present study, significant *LINC01426* upregulation was observed in NSCLC tissues and cell lines. Functional experiments showed that *LINC01426* knockdown markedly inhibited the proliferation, migration, and invasion of NSCLC cells and facilitated cell apoptosis in vitro. Furthermore, *LINC01426* interference restricted the growth of NSCLC tumors in vivo. These results suggest that *LINC01426* is a useful diagnostic and therapeutic target for NSCLC. But, *LINC01426* expression presented none correlation with tumor stage, overall survival or disease free survival in patients with NSCLC, implying that *LINC01426* may have no potential to be developed as a prognostic biomarker.

The subcellular localization of lncRNAs determines their mechanisms of action.[44] To elucidate the mechanisms involved in LINC01426-mediated control of NSCLC malignant behavior, the subcellular distribution of *LINC01426* was examined. Our study confirmed that *LINC01426* was primarily localized in the cytoplasm of NSCLC cells. Cytoplasmic lncRNAs are capable of sequestering miRNAs and decreasing their inhibitory effects on target genes.[45] Bioinformatics analysis was performed and the findings validated the relationship between miR-519d-5p and *LINC01426* by revealing that miR-519d-5p was significantly overexpressed in response to *LINC01426* depletion. Furthermore, an inverse correlation existed between *LINC01426* and miR-519d-5p expression in NSCLC tissues. In addition, the luciferase reporter and RIP assays revealed that *LINC01426* showed the ability to directly bind to miR-519d-5p and act as a molecular sponge for miR-519d-5p in NSCLC cells.

Further, mechanistic experiments revealed that *ETS1* is a direct target gene of miR-519d-5p in NSCLC cells.

According to the ceRNA theory, lncRNAs can compete for miRNA binding and consequently increase the target mRNA expression.[23] We evaluated the regulatory effect of *LINC01426* on *ETS1* expression in NSCLC cells. Our results indicated that *LINC01426* positively regulated *ETS1* expression in NSCLC cells by sequestering miR-519d-5p. These findings evidently demonstrate that a LINC01426/miR-519d-5p/ETS1 ceRNA pathway exists in NSCLC.

ETS1, a member of the ETS family of transcription factors, was shown to be the downstream target of miR-519d-5p. *ETS1* is a known oncogene that reportedly facilitates oncogenesis and development in NSCLC by attenuating several processes including proliferation, cell cycle, apoptosis, migration, invasion, tumor formation, chemosensitivity, angiogenesis, and epithelial–mesenchymal transition.[36–38] In the present study, mechanistic studies revealed a novel regulatory mechanism of the LINC01426/miR-519d-5p axis with respect to *ETS1*. MiR-519d-5p functions as a molecular bridge between *LINC01426* and *ETS1*, and the regulatory effect of *LINC01426* on *ETS1* expression is eliminated by miR-519d-5p. Moreover, the anti-oncogenic actions of *LINC01426* deficiency were offset by miR-519d-5p inhibition in NSCLC cells. Therefore, *LINC01426* can induce *ETS1* expression by sequestering miR-519d-5p, thereby aggravating malignant NSCLC progression.

In our study, we did not observe the metastasis in nude mice. It may be due to injection method and inadequate experiment period. Our study used subcutaneous injection. In the near future, we will employ the tail vein injection and longer experiment period to explore whether *LINC01426* can promote the metastasis of NSCLC cells in vivo.

Conclusion

The present study demonstrated the aberrantly high expression of *LINC01426* in NSCLC tissues and cell lines. *LINC01426* knockdown suppressed the tumorigenicity of NSCLC cells in vitro and in vivo. Preliminary experiments identified a LINC01426/miR-519d-5p/ETS1 ceRNA pathway in NSCLC cells, and *LINC01426* exerted oncogenic activity via the miR-519d-5p/ETS1 axis. The discovery of the LINC01426/miR-519d-5p/ETS1 pathway may lead to the identification of effective therapeutic targets for managing NSCLC.

Consent for Publication

Not applicable.

Disclosure

The authors report no conflicts of interest for this work.

References

1. Siegel RL, Miller KD, Jemal A. Cancer statistics, 2019. *CA Cancer J Clin*. 2019;69(1):7–34.
2. Bray F, Ferlay J, Soerjomataram I, Siegel RL, Torre LA, Jemal A. Global cancer statistics 2018: GLOBOCAN estimates of incidence and mortality worldwide for 36 cancers in 185 countries. *CA Cancer J Clin*. 2018;68(6):394–424.
3. Chen Z, Fillmore CM, Hammerman PS, Kim CF, Wong KK. Non-small-cell lung cancers: a heterogeneous set of diseases. *Nat Rev Cancer*. 2014;14(8):535–546. doi:10.1038/nrc37
4. Ramalingam SS, Owonikoko TK, Khuri FR. Lung cancer: new biological insights and recent therapeutic advances. *CA Cancer J Clin*. 2011;61(2):91–112.
5. Choe G, Horne R, Mollberg D. New Surgical Approaches in the Treatment of Non-Small Cell Lung Cancer. *Clin Chest Med*. 2020;41(2):173–183. doi:10.1016/j.ccm.2020.02.007
6. Zhang Y, Chen B, Wang L, Wang R, Yang X. Systemic immune-inflammation index is a promising noninvasive marker to predict survival of lung cancer: a meta-analysis. *Medicine*. 2019;98(3):e13788. doi:10.1097/MD.0000000000013788
7. Reck M, Heigener DF, Mok T, Soria JC, Rabe KF. Management of non-small-cell lung cancer: recent developments. *Lancet*. 2013;382(9893):709–719. doi:10.1016/S0140-6736(13)61502-0
8. Herbst RS, Morgensztern D, Boshoff C. The biology and management of non-small cell lung cancer. *Nature*. 2018;553(7689):446–454. doi:10.1038/nature25183
9. Fan C, Tang Y, Wang J, et al. Role of long non-coding RNAs in glucose metabolism in cancer. *Mol cancer*. 2017;16(1):130. doi:10.1186/s12943-017-0699-3
10. Kornienko AE, Guenzl PM, Barlow DP, Pauler FM. Gene regulation by the act of long non-coding RNA transcription. *BMC Biol*. 2013;11:59. 1 doi:10.1186/1741-7007-11-59
11. Quinn JJ, Chang HY. Unique features of long non-coding RNA biogenesis and function. *Nat Rev Genetics*. 2016;17(1):47–62. doi:10.1038/nrg.2015.10
12. Peng WX, Koirala P, Mo YY. LncRNA-mediated regulation of cell signaling in cancer. *Oncogene*. 2017;36(41):5661–5667. doi:10.1038/onc.2017.184
13. Guzel E, Okyay TM, Yalcinkaya B, Karacaoglu S, Gocmen M, Akcakuyu MH. Tumor suppressor and oncogenic role of long non-coding RNAs in cancer. *Northern Clin Istanbul*. 2020;7(1):81–86.
14. Liu K, Gao L, Ma X, et al. Long non-coding RNAs regulate drug resistance in cancer. *Mol Cancer*. 2020;19(1):54. doi:10.1186/s12943-020-01162-0
15. Zhang HD, Jiang LH, Zhong SL, et al. The role of long non-coding RNAs in drug resistance of cancer. *Clin Genetics*. 2020. doi:10.1111/cge.13800
16. Chen Z, Lei T, Chen X, et al. Long non-coding RNA in lung cancer. *Clinica Chimica Acta*. 2020;504:190–200. doi:10.1016/j.cca.2019.11.031
17. Moises J, Navarro A, Castellano JJ, et al. Long non-coding RNA NANCI/NKX2-1 duplex impacts prognosis in Stage I non-small-cell lung cancer. *Arch Bronconeumol*. 2020.
18. Shen J, Ma J, Li J, Wang X, Wang Y, Ma J. A long non-coding RNA LNBC3 facilitates non-small cell lung cancer progression by stabilizing BCL6. *J Clin Lab Anal*. 2020;34(4):e23122. doi:10.1002/jcla.23122

19. Wu KL, Tsai YM, Lien CT, Kuo PL, Hung AJ. The roles of MicroRNA in lung cancer. *Int J Mol Sci*. 2019;20:7.
20. Kim VN. MicroRNA biogenesis: coordinated cropping and dicing. *Nat Rev Molecular Cell Biol*. 2005;6(5):376–385. doi:10.1038/nrm1644
21. Petrek H, Yu AM. MicroRNAs in non-small cell lung cancer: Gene regulation, impact on cancer cellular processes, and therapeutic potential. *Pharmacol Res Perspectives*. 2019;7(6):e00528. doi:10.1002/prp2.528
22. Weidle UH, Birzele F, Nopora A. MicroRNAs as Potential Targets for Therapeutic Intervention With Metastasis of Non-small Cell Lung Cancer. *Cancer Genomics Proteomics*. 2019;16(2):99–119. doi:10.21873/cgp.20116
23. Qu J, Li M, Zhong W, Hu C. Competing endogenous RNA in cancer: a new pattern of gene expression regulation. *Int J Clin Exp Med*. 2015;8(10):17110–17116.
24. Abdollahzadeh R, Daraei A, Mansoori Y, Sepahvand M, Amoli MM, Tavakkoly-Bazzaz J. Competing endogenous RNA (ceRNA) cross talk and language in ceRNA regulatory networks: a new look at hallmarks of breast cancer. *J Cell Physiol*. 2019;234(7):10080–10100. doi:10.1002/jcp.27941
25. Wang SJ, Wang H, Zhao CD, Li R. Long noncoding RNA LINC01426 promotes glioma progression through PI3K/AKT signaling pathway and serves as a prognostic biomarker. *Eur Rev Med Pharmacol Sci*. 2018;22(19):6358–6368.
26. Cao J, Tang Z, Su Z. Long non-coding RNA LINC01426 facilitates glioblastoma progression via sponging miR-345-3p and upregulation of VAMP8. *Cancer Cell Int*. 2020;20:327. doi:10.1186/s12935-020-01416-3
27. Jiang Y, Zhang H, Li W, Yan Y, Yao X, Gu W. LINC01426 contributes to clear cell renal cell carcinoma progression by modulating CTBP1/miR-423-5p/FOXM1 axis via interacting with IGF2BP1. *J Cell Physiol*. 2020. doi:10.1002/jcp.29871
28. Tian B, Han X, Li G, et al. A Long Intergenic Non-coding RN[illegible] LINC01426, Promotes Cancer Progression via AZGP1 and Predicts Poor Prognosis in Patients with LUAD. *Mol Ther Methods Clin Develop*. 2020;18:765–780. doi:10.1016/j.omtm.2020[illegible].001
29. Ye Y, Zhao L, Li Q, Xi C, Li Y, Li Z. circ [illegible]7385 served as competing endogenous RNA for miR-519d-3p to suppress [illegible] behaviors and cisplatin resistance of non-sm[illegible] cell l[illegible]ncer cells. *Thoracic Cancer*. 2020. 11 8 219[illegible]2208 doi:[illegible]1111/1759-7714.13527
30. Lv B, Li F, Liu X, Lin L. [illegible]e tum[illegible] suppressive [illegible]ole of microRNA-873 in nasopharyng[illegible]l carcinoma [illegible]relates with down-regulation of ZIC2 and inhib[illegible]on of AKT signalin[illegible]athway. *Cancer Gene Ther*. 2020. doi:10.[illegible]38/s41417-020-0185-8
31. Feng J, Wang T. Mic[illegible]NA-87[illegible]erves a critical role in human cervical cancer prolife[illegible]r and me[illegible]tasis via regulating glioma-associate[illegible]gene [illegible]molog 1. *Exp Ther Med*. 2020;19(2):1243–125[illegible]
32. Tan Z, Cao F, Jia B, Xia L. Circ_0072088 promotes the development of non-small cell lung cancer via the miR -377-5p/ NOVA2 axis. *Thoracic Cancer*. 2020. 11 8 2224–2236 doi:10.1111/1759-7714.13529
33. Wu H, Liu HY, Liu WJ, Shi YL, Bao D. miR-377-5p inhibits lung cancer cell proliferation, invasion, and cell cycle progression by targeting AKT1 signaling. *J Cell Biochem*. 2018.
34. Zheng S, Wan L, Ge D, et al. LINC00266-1/miR-548c-3p/SMAD2 feedback loop stimulates the development of osteosarcoma. *Cell Death Dis*. 2020;11(7):576. doi:10.1038/s41419-020-02764-8
35. Du Y, Zhu J, Chu BF, Yang YP, Zhang SL. MiR-548c-3p suppressed the progression of papillary thyroid carcinoma via inhibition of the HIF1alpha-mediated VEGF signaling pathway. *Eur Rev Med Pharmacol Sci*. 2019;23(15):6570–6578.
36. Yang YB, Tan H, Wang Q. MiRNA-300[illegible]ses proliferation, migration and invasion of non-small c[illegible] lung can[illegible] via targeting ETS1. *Eur Rev Med Pharmacol Sci*[illegible]19;23(24):108[illegible]10834.
37. Lou Z, Lee BS, Ha T, et al. ESE1 su[illegible]esses the gro[illegible]h, invasion and migration of human NSC[illegible] cells an[illegible]umor form[illegible]ion in vivo. *Oncol Rep*. 2018;40(3):173[illegible]1742.
38. Geng H, Li S, Xu M. Lo[illegible] Noncodi[illegible]RNA SN[illegible]o Functions as an Oncogene in Non-Small[illegible]ll L[illegible]g Cancer via Modulating ETS1 Signaling. *OncoTargets Ther*[illegible]020;13:92[illegible]930. doi:10.2147/OTT.S235336
39. Ye Y, Gu[illegible] Liu[illegible] et al. Long[illegible]on-Coding RNA SPRY4-IT1 Reverses Cisplatin [illegible]istance by Downregulating MPZL-1 via Suppr[illegible] EMT in [illegible]CLC. *OncoTargets Ther*. 2020;13:27[illegible]793. doi:10.2147/OTT.[illegible]232769
40. [illegible]ng B, Wang Y, Ma D, Wang L, Yang M. Long noncoding RNA [illegible]TS5 inhibits [illegible]on-small cell lung cancer by interacting with I[illegible]80. *Life Sci*.[illegible]020;253:117680. doi:10.1016/j.lfs.2020.117680
41. Feng [illegible], Yang[illegible], Zhou S, Deng S, Xie Y. Long non-coding RNA DDX11-AS1 promotes non-small cell lung cancer development via [illegible]ting PI3K/AKT signalling. *Clin Exp Pharmacol Physiol*. 2020. 47 9 1622–1631 doi:10.1111/1440-1681.13325
42. Yang H, Yang W, Dai W, Ma Y, Zhang G. LINC00667 promotes the proliferation, migration, and pathological angiogenesis in non-small cell lung cancer through stabilizing VEGFA by EIF4A3. *Cell Biol Int*. 2020;44(8):1671–1680. doi:10.1002/cbin.11361
43. Li L, Wang Y, Zhang X, et al. Long non-coding RNA HOXD-AS1 in cancer. *Clinica Chimica Acta*. 2018;487:197–201. doi:10.1016/j.cca.2018.10.002
44. Chan JJ, Tay Y. Noncoding RNA:RNA Regulatory Networks in Cancer. *Int J Mol Sci*. 2018;19:5. doi:10.3390/ijms19051310
45. Yuan T, Huang X, Dittmar RL, et al. eRNA: a graphic user interface-based tool optimized for large data analysis from high-throughput RNA sequencing. *BMC Genomics*. 2014;15:176. doi:10.1186/1471-2164-15-176